Asymmetric Neutral Gas Shielding model for the pellet rocket force

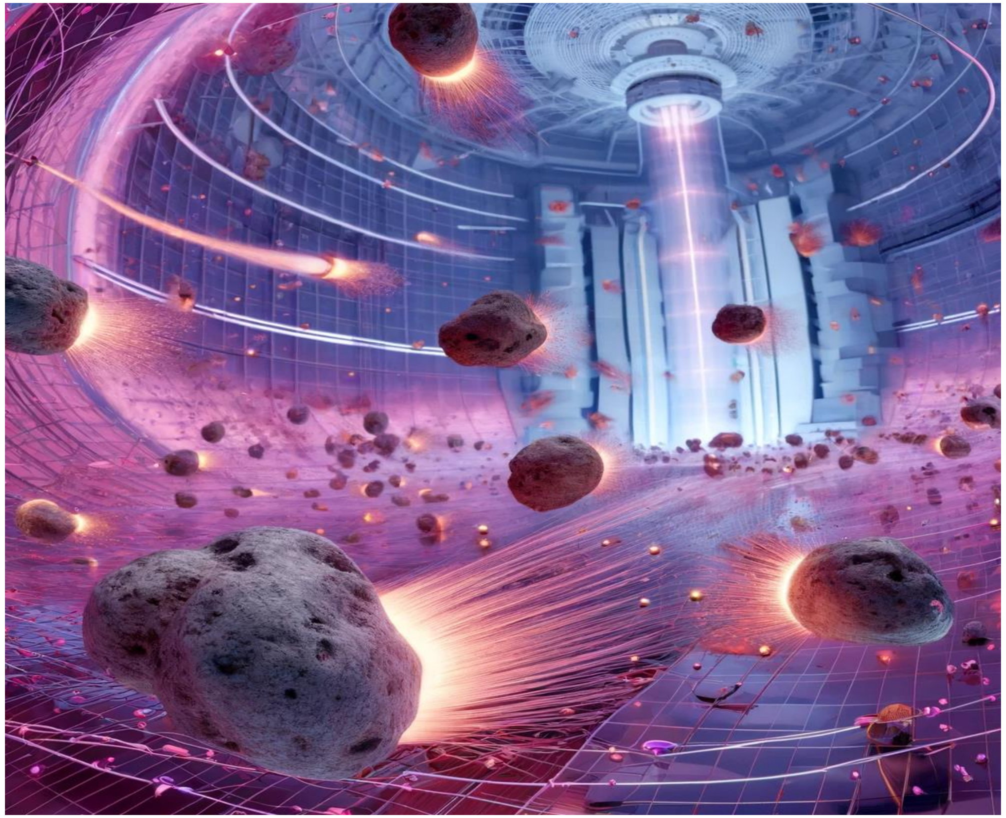

Oskar Vallhagen

Nico Guth, Per Helander, Tünde Fülöp, Amir Tresnjic,
Sarah Newton, István Pusztai

Asymmetric heating leads to rocket force

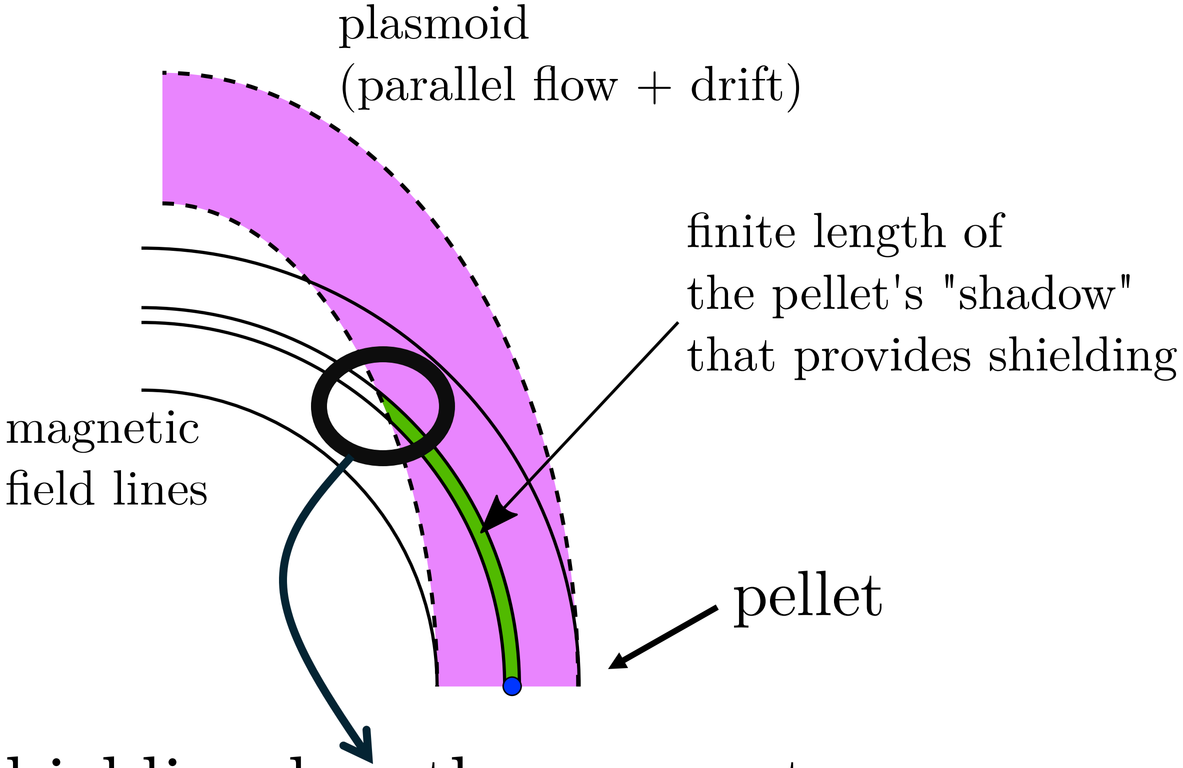

shielding length asymmetry,
n, T gradients
=> asymmetric heating

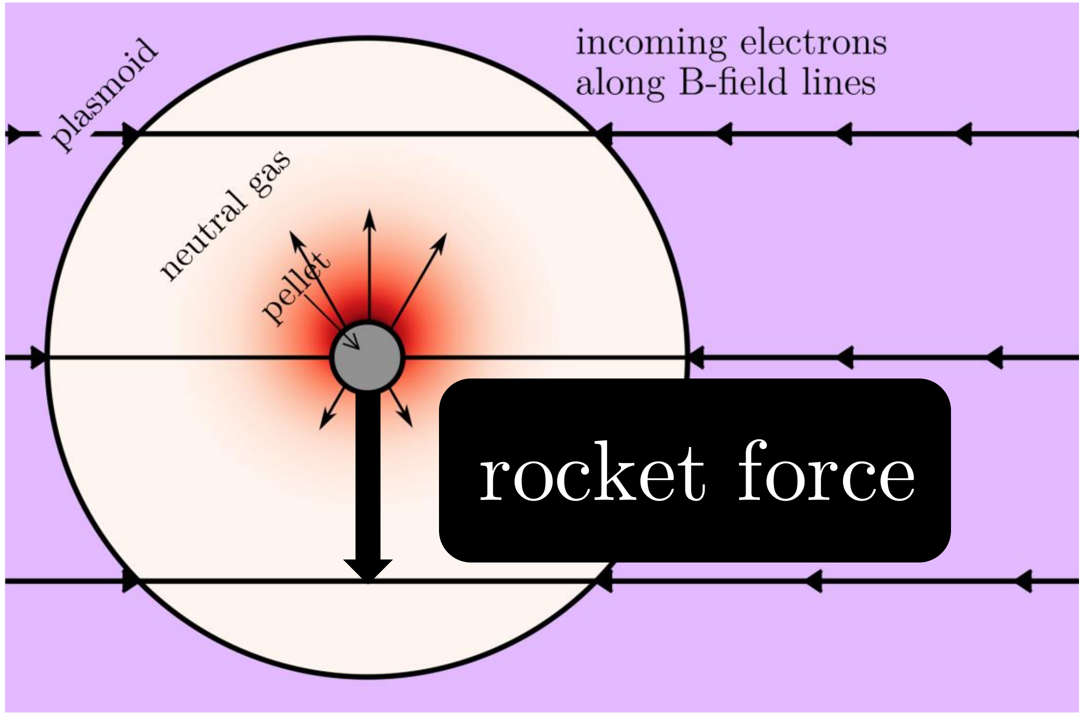

Force on pellet surface

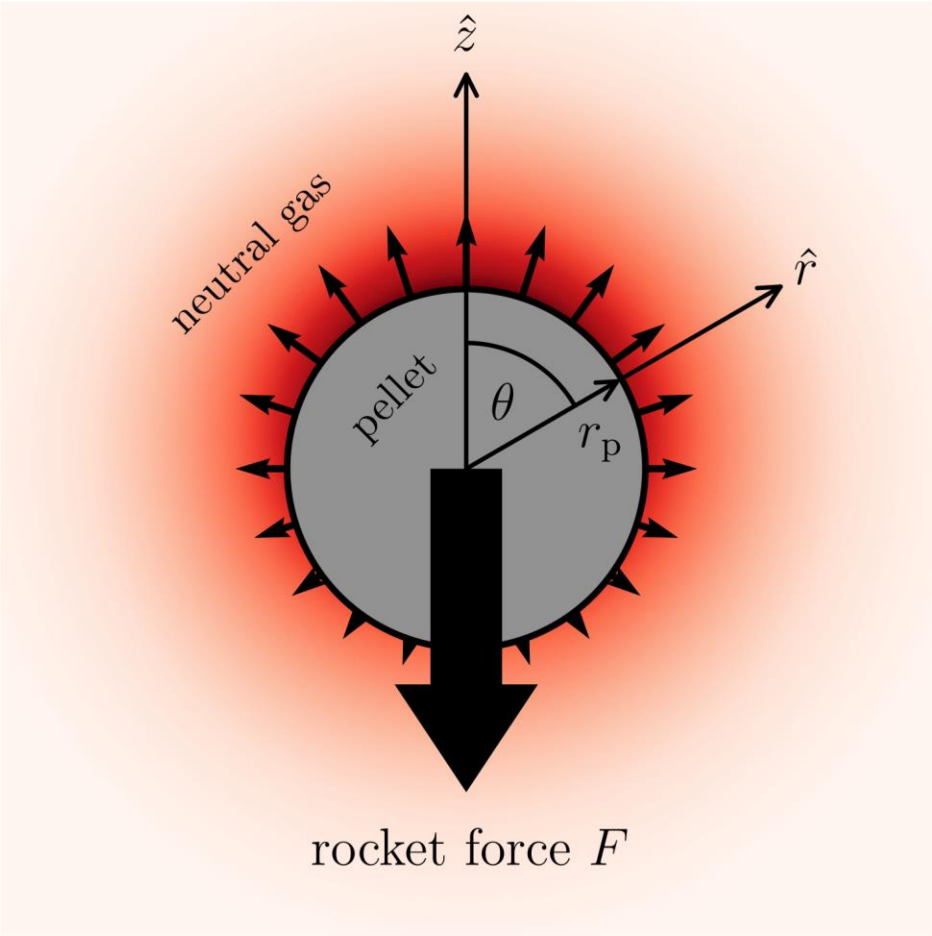

- Momentum transfer:

$$\vec{F} = -\iint_S \overleftrightarrow{\Pi} \cdot \mathrm{d}\vec{S}$$

- Expand in spherical harmonics

$$p(r,\theta,\phi) = p_0(r) + p_1(r)\cos\theta + \ldots$$
$$\rho(r,\theta,\phi) = \rho_0(r) + \rho_1(r)\cos\theta + \ldots$$

- Result for cryogenic pellet:

$$F = \frac{4\pi r_{\mathrm{p}}^2}{3} p_1(r_{\mathrm{p}})$$

Neutral gas shielding (NGS)

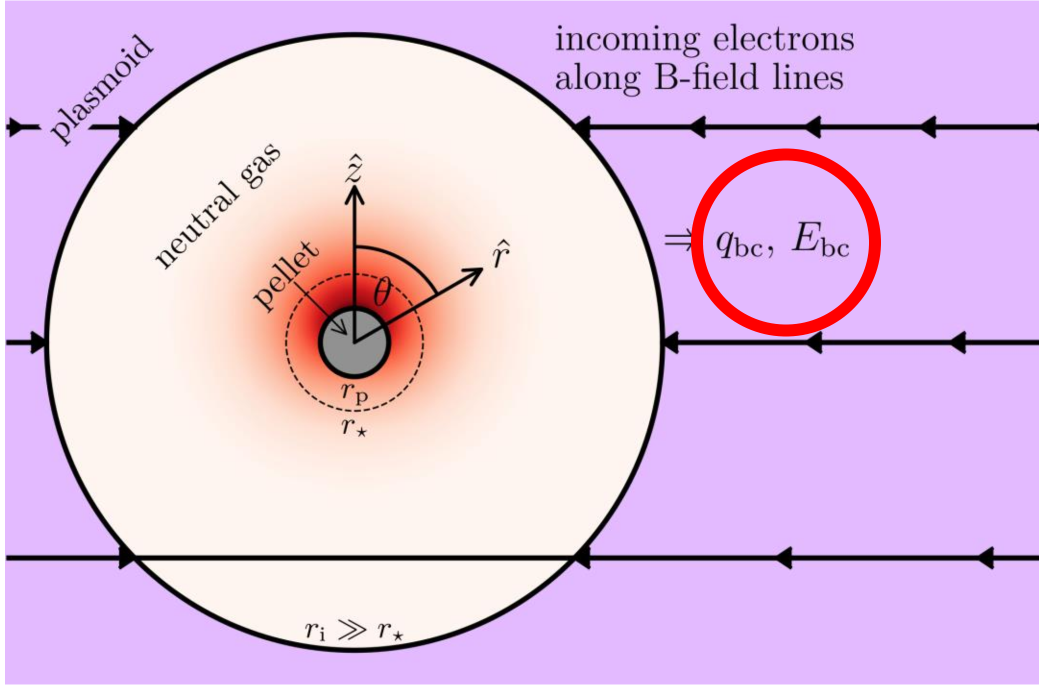

- Quasi steady-state ideal gas balance equations:

$$\frac{\rho}{m} = \frac{p}{T} \qquad \text{(ideal gas law)}$$

$$\vec{\nabla} \cdot (\rho \vec{v}) = 0 \qquad \text{(mass)}$$

$$\rho(\vec{v} \cdot \vec{\nabla})\vec{v} = -\vec{\nabla} p \qquad \text{(momentum)}$$

$$\vec{\nabla} \cdot \left[\left(\frac{\rho v^2}{2} + \frac{\gamma p}{\gamma - 1} \right) \vec{v} \right] = Q \qquad \text{(energy)}$$

Neutral gas shielding (NGS)

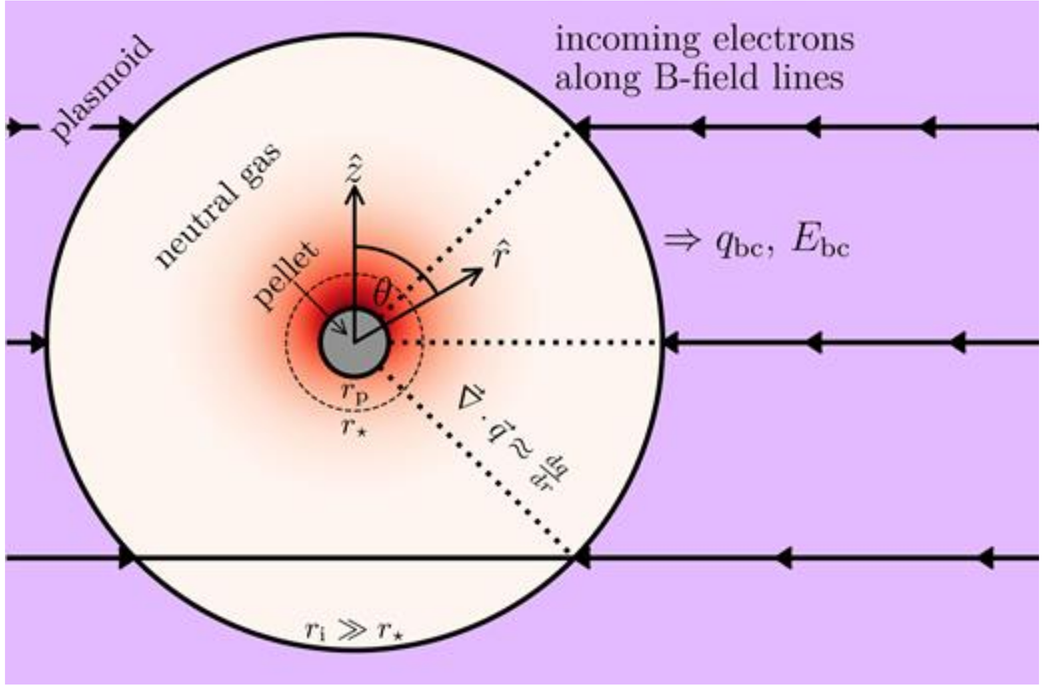

- Electron heating approximations:
  - Mono-energetic beam
  - Equivalent radial path
  - Empirical energy loss functions
  - Fully shielded
- Heating asymmetry parameters

$$q_{\mathrm{rel}} = \frac{q_1(\infty)}{q_0(\infty)} \quad \text{and} \quad E_{\mathrm{rel}} = \frac{E_1(\infty)}{E_0(\infty)}$$

- Small asymmetric perturbation -> linearise

Normalized equation system

- Complicated, but still linear 1D ODE system
- Normalization -> semi-analytical

$$\widetilde{p}_0 = \frac{p_0}{p_\star}, \quad \widetilde{p}_1 = \frac{p_1}{p_\star q_{\rm rel}}, \ldots$$

- Normalized solution parameters

$$\gamma, \quad E_{\rm bc}, \quad \frac{E_{\rm rel}}{q_{\rm rel}}$$

$$\frac{\partial}{\partial r}\left(\frac{p_0}{T_0}\right) v_{1,r} + \frac{p_0}{T_0}\frac{1}{r^2}\frac{\partial}{\partial r}\left(r^2 v_{1,r}\right) + v_0 \frac{\partial}{\partial r}\left(\frac{p_1}{T_0} - \frac{p_0}{T_0^2}T_1\right) + \frac{1}{r^2}\frac{\partial}{\partial r}\left(r^2 v_0\right)\left(\frac{p_1}{T_0} - \frac{p_0}{T_0^2}T_1\right) -$$
$$2\frac{p_0}{rT_0}v_{1,\theta} = 0$$

$$\frac{p_0}{T_0}v_{1,r}v_0' + \frac{p_0}{T_0}v_0 U_1' + \left(\frac{p_1}{T_0} - \frac{p_0}{T_0^2}T_1\right) v_0 v_0' + \frac{P_1'}{\gamma} = 0$$

$$\frac{p_0}{T_0}\frac{v_0}{r}v_{1,\theta} + \frac{p_0}{T_0}v_0 V_1' + \frac{P}{\gamma r} = 0$$

$$\left(\frac{p_0 v_0^2}{2T_0} + \frac{p_0}{\gamma - 1}\right)\left[\frac{1}{r^2}\frac{\partial}{\partial r}\left(r^2 v_{1,r}\right) - 2\frac{v_{1,\theta}}{r}\right] + v_{1,r}\frac{\partial}{\partial r}\left(\frac{p_0 v_0^2}{2T_0} + \frac{p_0}{\gamma - 1}\right) +$$
$$\left[\left(\frac{p_1}{T_0} - \frac{p_0}{T_0^2}T_1\right)\frac{v_0^2}{2} + \frac{p_0}{T_0}v_0 v_{1,r} + \frac{p_1}{\gamma - 1}\right]\frac{1}{r^2}\frac{\partial}{\partial r}\left(r^2 v_0\right) +$$
$$v_0 \frac{\partial}{\partial r}\left[\left(\frac{p_1}{T_0} - \frac{p_0}{T_0^2}T_1\right)\frac{v_0^2}{2} + \frac{p_0}{T_0}v_0 v_{1,r} + \frac{p_1}{\gamma - 1}\right] = \frac{2}{(\gamma - 1)\lambda_*}\frac{\partial q_1}{\partial r}$$

$$\frac{\partial q_1}{\partial r} = \lambda_* \left[\left(\frac{p_1}{T_0} - \frac{p_0}{T_0^2}T_1\right) q_0 \Lambda(E_0) + \frac{p_0}{T_0}q_0 \left.\frac{d\Lambda}{dE}\right|_{E=E_0} E_1 + \frac{p_0}{T_0}\Lambda(E_0) q_1\right]$$

$$\frac{\partial E_1}{\partial r} = 2\lambda_* \left[\left(\frac{p_1}{T_0} - \frac{p_0}{T_0^2}T_1\right) L(E_0) + 2\frac{p_0}{T_0}\left.\frac{dL}{dE}\right|_{E=E_0} E_1\right]$$

$$T_1(r_p) = 0, \quad q_1(r_p) = 0,$$
$$p_1(\infty) = 0, \quad q_1(\infty) = q_0(\infty), \quad E_1(\infty) = E_0(\infty) E_{\rm rel}/q_{\rm rel}$$

Pressure asymmetry at pellet surface

$$p(\vec{r}) = p_0(r) + p_1(r)\cos\theta + \dots$$

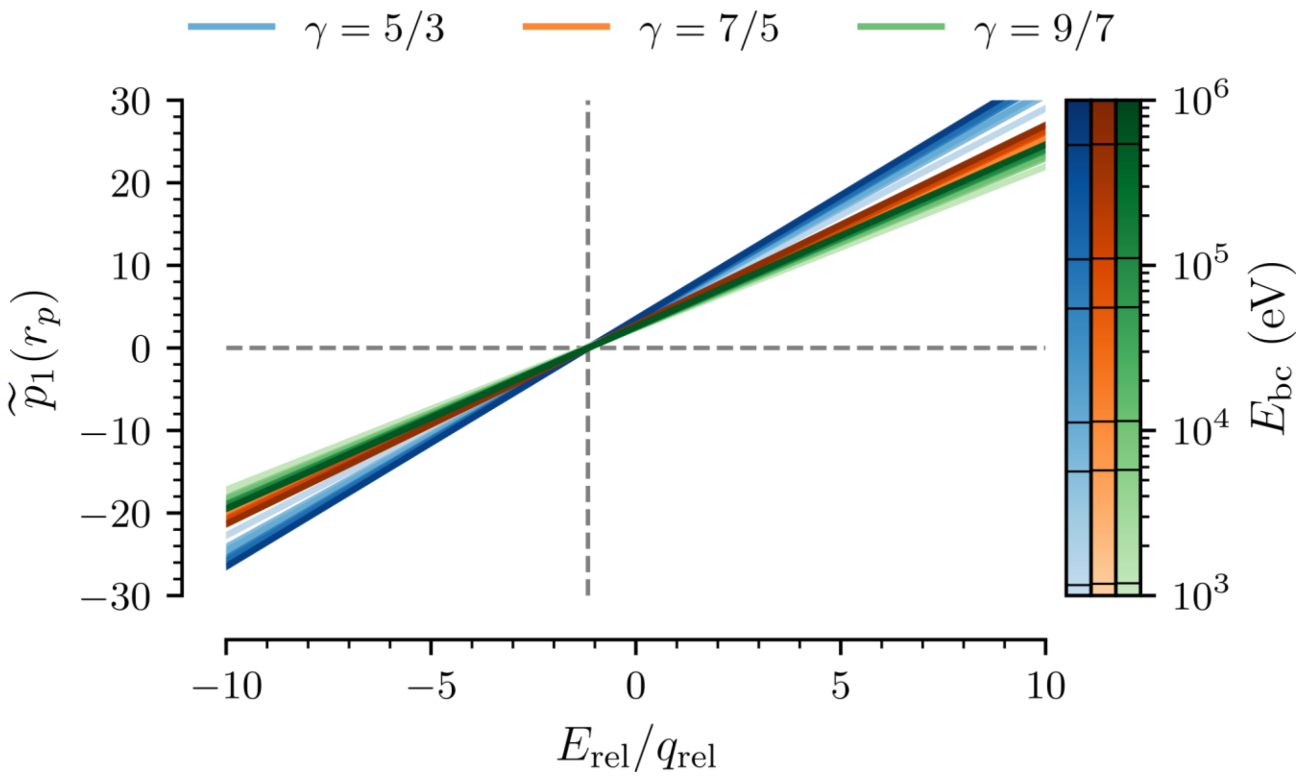

- Linear dependence on $E_{\rm rel}/q_{\rm rel}$
- Weak dependence on $\gamma, E_{\rm bc}$
- Final rocket force:

$$\boxed{F = \frac{4\pi r_{\rm p}^2}{3}\underbrace{p_\star\left(aE_{\rm rel} + abq_{\rm rel}\right)}_{p_1(r_{\rm p})}}$$

$a \approx 2.0$ to 2.9
$b \approx -1.17$ to -1.21

- Without plasmoid shielding:

$$q_{\rm rel} = \frac{3}{2}\frac{r_{\rm p}}{T_{\rm bg}}\frac{dT_{\rm bg}}{dz} + \frac{r_{\rm p}}{n_{\rm bg}}\frac{dn_{\rm bg}}{dz}$$

$$E_{\rm rel} = \frac{r_{\rm p}}{T_{\rm bg}}\frac{dT_{\rm bg}}{dz}$$

Plasmoid shielding asymmetry

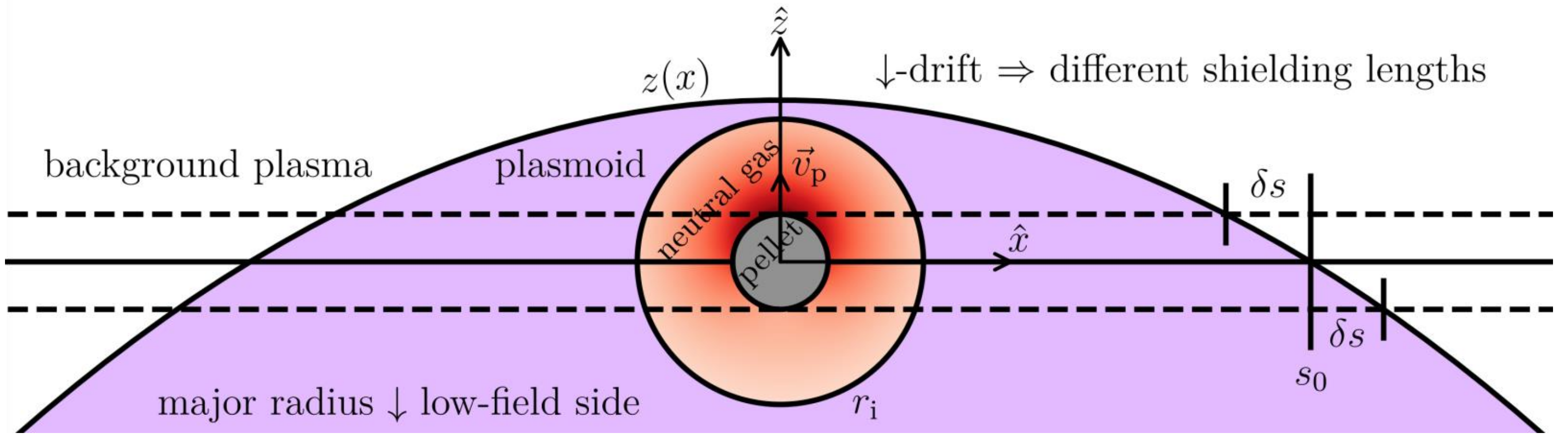

Plasmoid boundary:

- Expansion at speed of sound
- Constant drift acceleration (Vallhagen, 2023)

$$\dot{v}_{\mathrm{pl}} = \frac{2(1+\langle Z\rangle)}{\langle m_i\rangle R_{\mathrm{m}}}\left(T_{\mathrm{pl}} - \frac{2n_{\mathrm{bg}}}{(1+\langle Z\rangle)n_{\mathrm{pl}}}T_{\mathrm{bg}}\right)$$

- Gives trajectory of boundary determining shielding length:

$$\vec{r}(t) = (\pm c_{\mathrm{s}}t)\hat{x} + \left(r_{\mathrm{i}} - v_{\mathrm{p}}t - \frac{1}{2}\dot{v}_{\mathrm{pl}}t^2\right)\hat{z}$$

Plasmoid shielding asymmetry

Shielding assumptions:

- Electron stopped when path length > mean free path

$$d = \frac{s}{\xi} < \lambda_{\mathrm{mfp}} \Rightarrow v_{\mathrm{c}} = \left(\frac{s}{\xi \lambda_T}\right)^{\frac{1}{4}} v_{\mathrm{th}}$$

- Density from mass conservation

$$n_{\mathrm{pl}} = \frac{\mathcal{G}}{2\langle m_i \rangle c_{\mathrm{s}}(T_{\mathrm{pl}}) \pi r_{\mathrm{i}}^2}$$

- Temperature close to ionization threshold (about 2 eV)
- Assume cross-section absorbs energy needed for full ionization

$$r_{\mathrm{i}} = \sqrt{\frac{\mathcal{G}(4\gamma T_{\mathrm{pl}} + \varepsilon_{\mathrm{ion}} + \varepsilon_{\mathrm{diss}})}{m_i \pi q_{\mathrm{bg}}}}$$

Pellet trajectory simulation in AUG

- Coupled ablation rate and rocket force equations
- Fix background plasma profiles
  - Material drifts away from pellet
- Profiles similar to Szepesi et al, Journal of Nucl. Mat. 2009

  $\#23078, \quad T_{\max} \approx 0.6\,\mathrm{keV}, \quad n_{\max} \approx 10^{20}\,\mathrm{m}^{-3}$
- Agrees reasonably well with AUG experiment
- Shielding asymmetry dominates

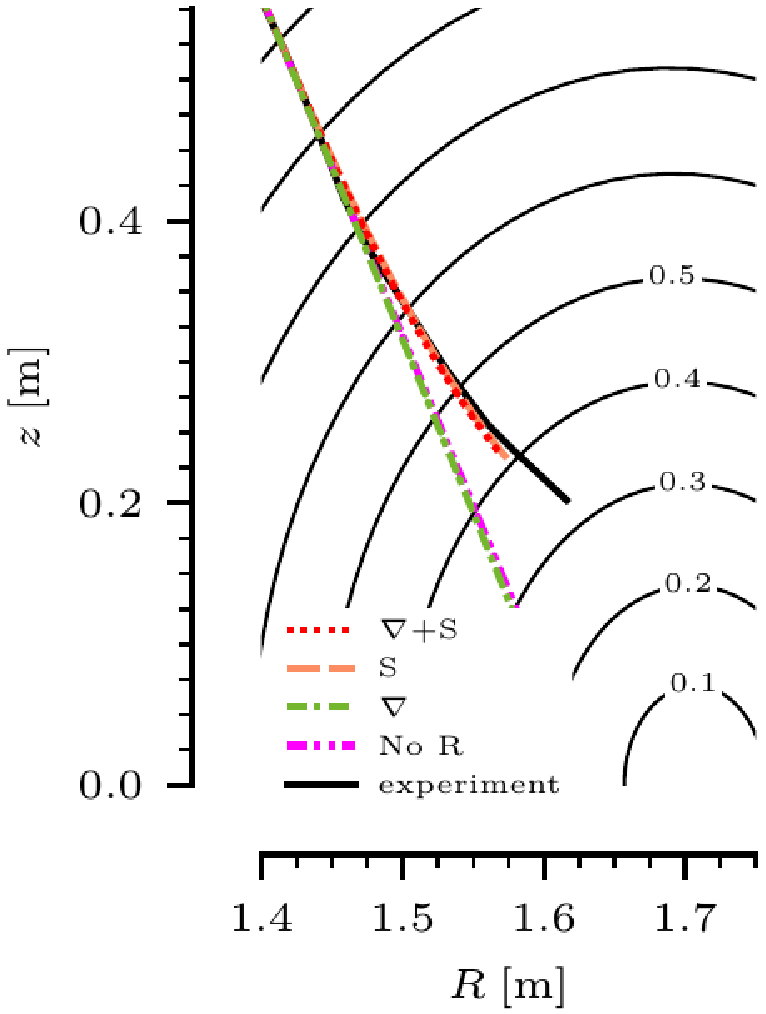

Penetration depth in ITER

- Generally higher impact than in present day devices
  - Higher temperature, higher pedestal => stronger rocket force
- Small penetration depths even without rocket force in H-mode
  - Need cumulative effect of SPI shards (or HFS injection)
- Only moderate effect of shielding
  - Decrease with ionization radius, shielding dampens ablation rate

H26, $T_{\max} \approx 5\,\mathrm{keV}$, $n_{\max} \approx 5 \cdot 10^{19}\,\mathrm{m}^{-3}$

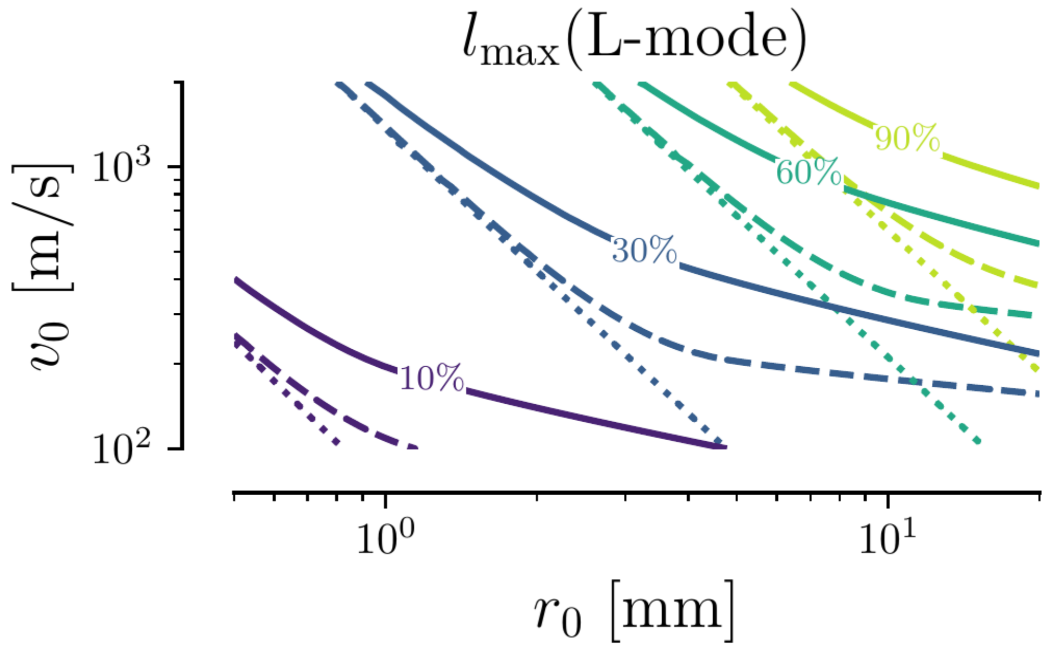

DTHmode24, $T_{\max} \approx 22\,\mathrm{keV}$, $n_{\max} \approx 10^{20}\,\mathrm{m}^{-3}$

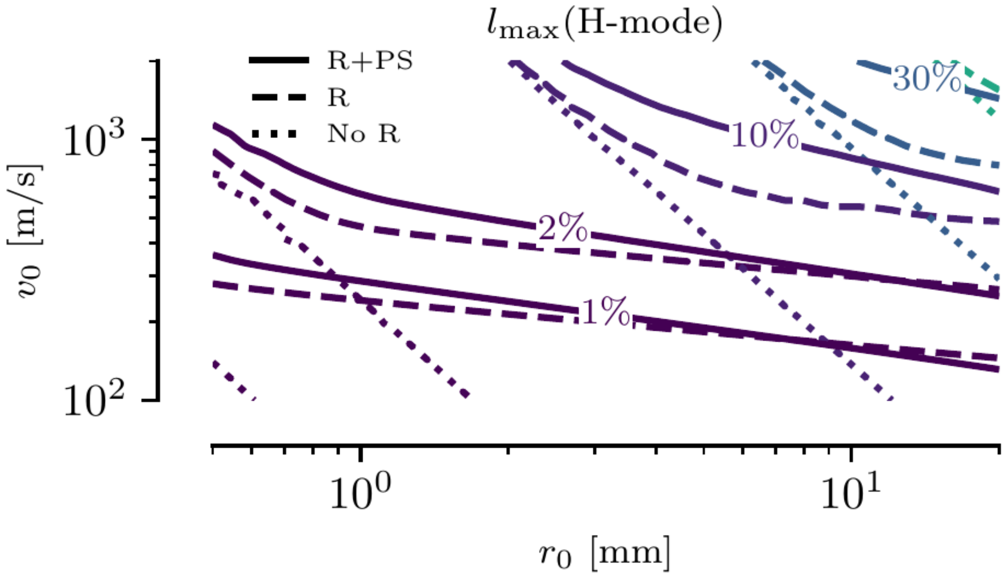

Conclusion

Summary

- Developed a self-consistent semi-analytical model for the pellet rocket effect
- Asymmetric NGS model
- Reasonable agreement with AUG experiments
- Could limit penetration depth in ITER, at least in H-mode

Outlook

- Improve on approximations
  - Plasmoid shielding, ionization radius
  - Mono-energetic beam
  - Radial electron path
- Include in self-consistent background plasma model
  - Study effect on SPI with several shards

Backup slides

Deflection of pellet shards in experiments

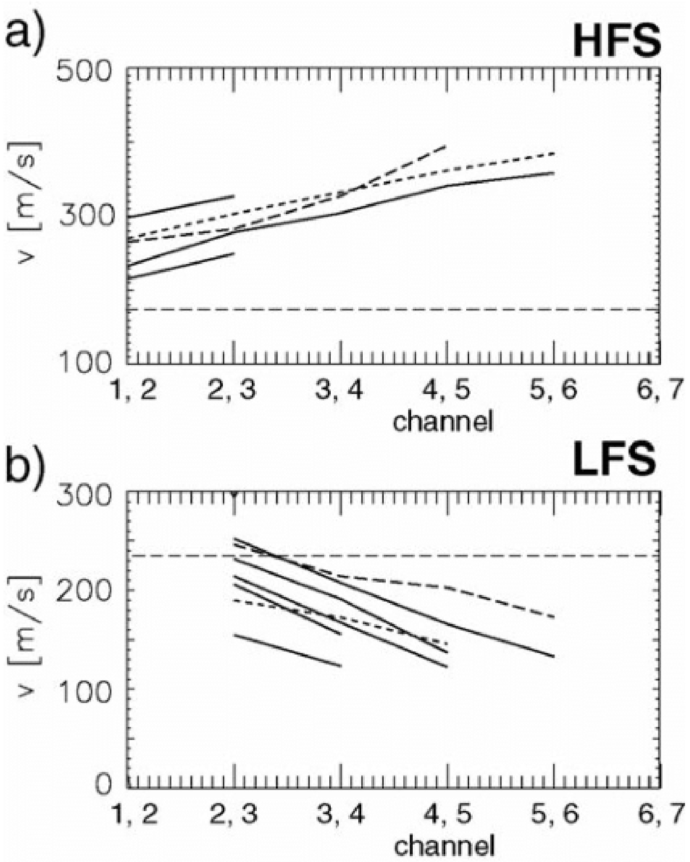

Pellet speed measurements in AUG (Müller et al NF 2002)

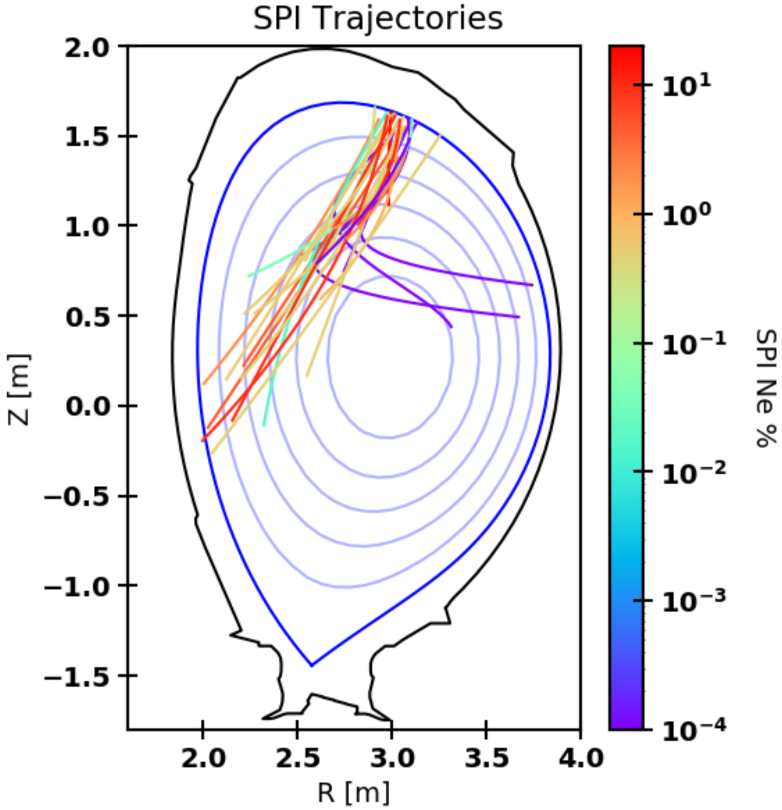

Pellet shard trajectories in JET (Umar Sheikh, private communication)

Modelling the pellet rocket effect

Previous models

- by Senichenkov et al. (2007)
  - only ablation asymmetry (no pressure)
  - simplified plasmoid drift and ablation model
- by Szepesi et al. (2007)
  - pressure asymmetry as semi-empirical parameter
- by Samulyak et al. (2023)
  - 3D Lagrangian particle code

Force on pellet surface

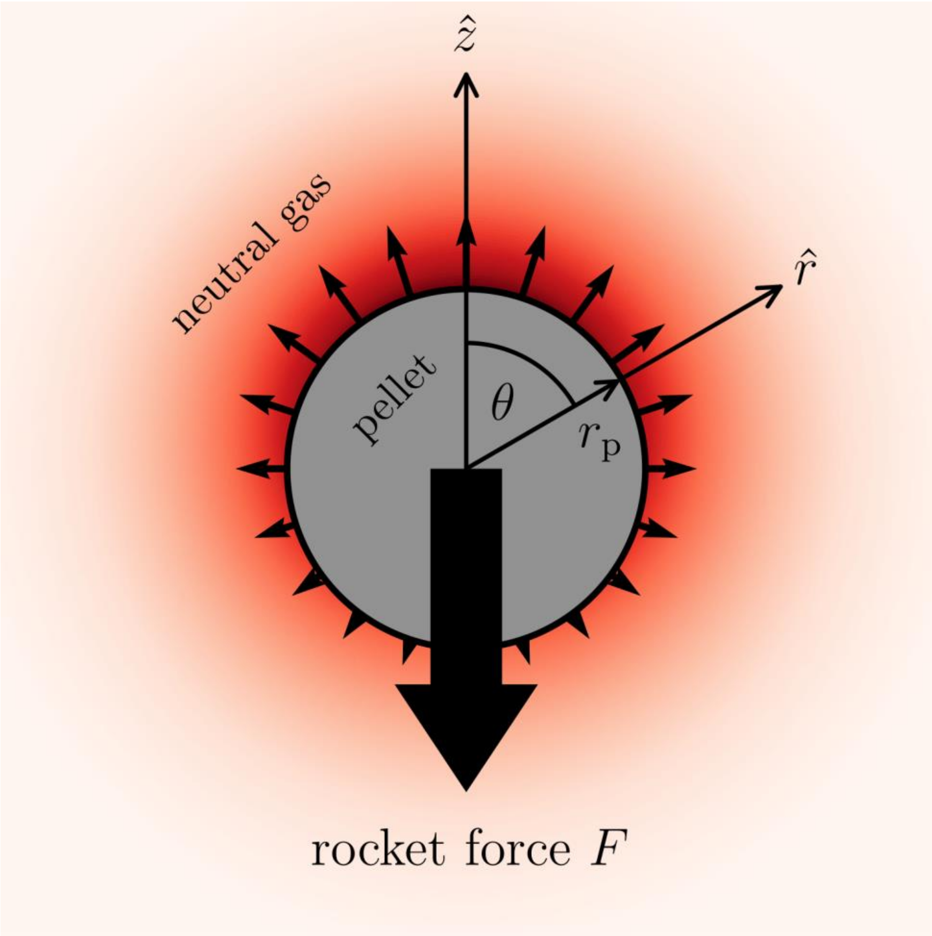

- Spherical harmonics expansion:

$$\delta\rho\,(r,\theta,\varphi) = \rho_1(r)\cos\theta + \dots\,,$$
$$\delta v_r\,(r,\theta,\varphi) = v_{1,r}(r)\cos\theta + \dots\,,$$

- Resulting force:

$$\boxed{F = \frac{4\pi r_\mathrm{p}^2}{3}\left(\rho_1 v_0^2 + 2\rho_0 v_0 (v_{1,r} - v_{1,\theta}) + p_1\right)_{r=r_\mathrm{p}}}$$

- For cryogenic pellets:

$$F = \frac{4\pi r_\mathrm{p}^2}{3} p_1(r_\mathrm{p})$$

Empirical energy attenuation

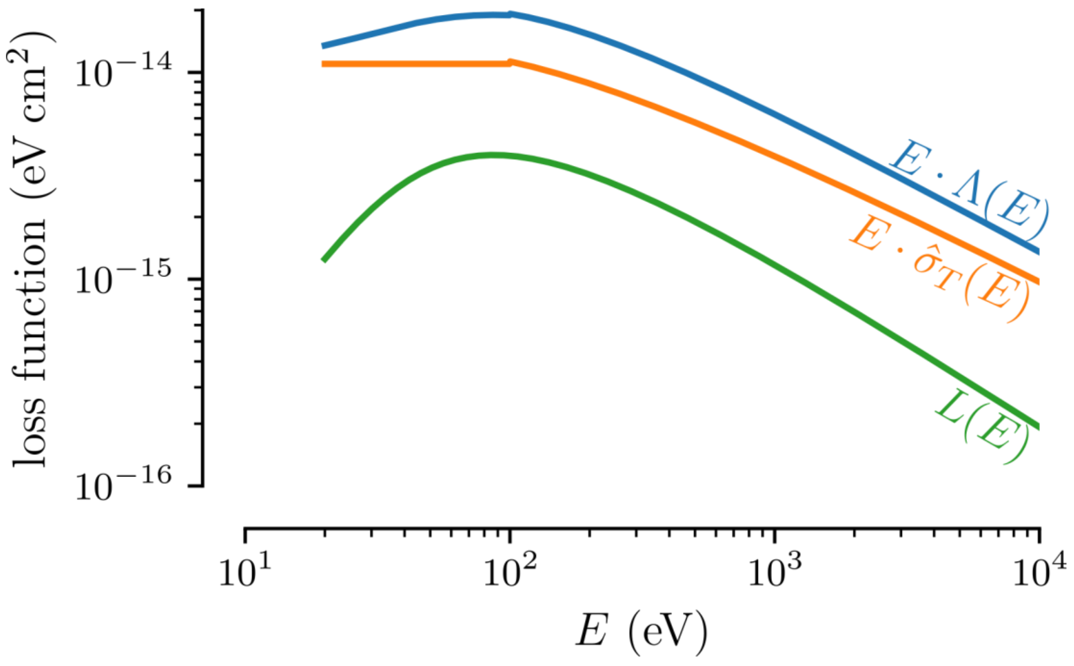

$$\Lambda(E) = \hat{\sigma}_T(E) + 2L(E)/E,$$

$$L(E > 20\,\text{eV}) = \frac{8.62 \times 10^{-15}\,\text{eV}\,\text{cm}^2}{\left(\frac{E/\text{eV}}{100}\right)^{0.823} + \left(\frac{E/\text{eV}}{60}\right)^{-0.125} + \left(\frac{E/\text{eV}}{48}\right)^{-1.94}}$$

$$\hat{\sigma}_T(E) = \begin{cases} \left(\dfrac{8.8 \times 10^{-13}}{(E/\text{eV})^{1.71}} - \dfrac{1.62 \times 10^{-12}}{(E/\text{eV})^{1.932}}\right)\text{cm}^2 & \text{for } E > 100\,\text{eV} \\ \left(\dfrac{1.1 \times 10^{-14}}{(E/\text{eV})}\right)\text{cm}^2 & \text{for } E < 100\,\text{eV} \end{cases}$$

$$\frac{\mathrm{d}E}{\mathrm{d}r} = 2\frac{\rho}{m}L(E)$$

$$\frac{\mathrm{d}q}{\mathrm{d}r} = \frac{q}{\lambda_{\text{mfp}}(E)} = \frac{\rho}{m}q\Lambda(E)$$

Isotropic NGS solutions

- ablation rate:

$$4\pi r^2 \frac{\rho}{m} v = const = G$$

- speed of sound:

$$v_\star = \sqrt{\frac{\gamma T_\star}{m}}$$

- normalization:

$$\tilde{\rho} = \frac{\rho}{\rho_\star}, \quad \tilde{p} = \frac{p}{p_\star}, \quad \tilde{T} = \frac{T}{T_\star}, \quad \tilde{v} = \frac{v}{v_\star}, \quad \ldots$$

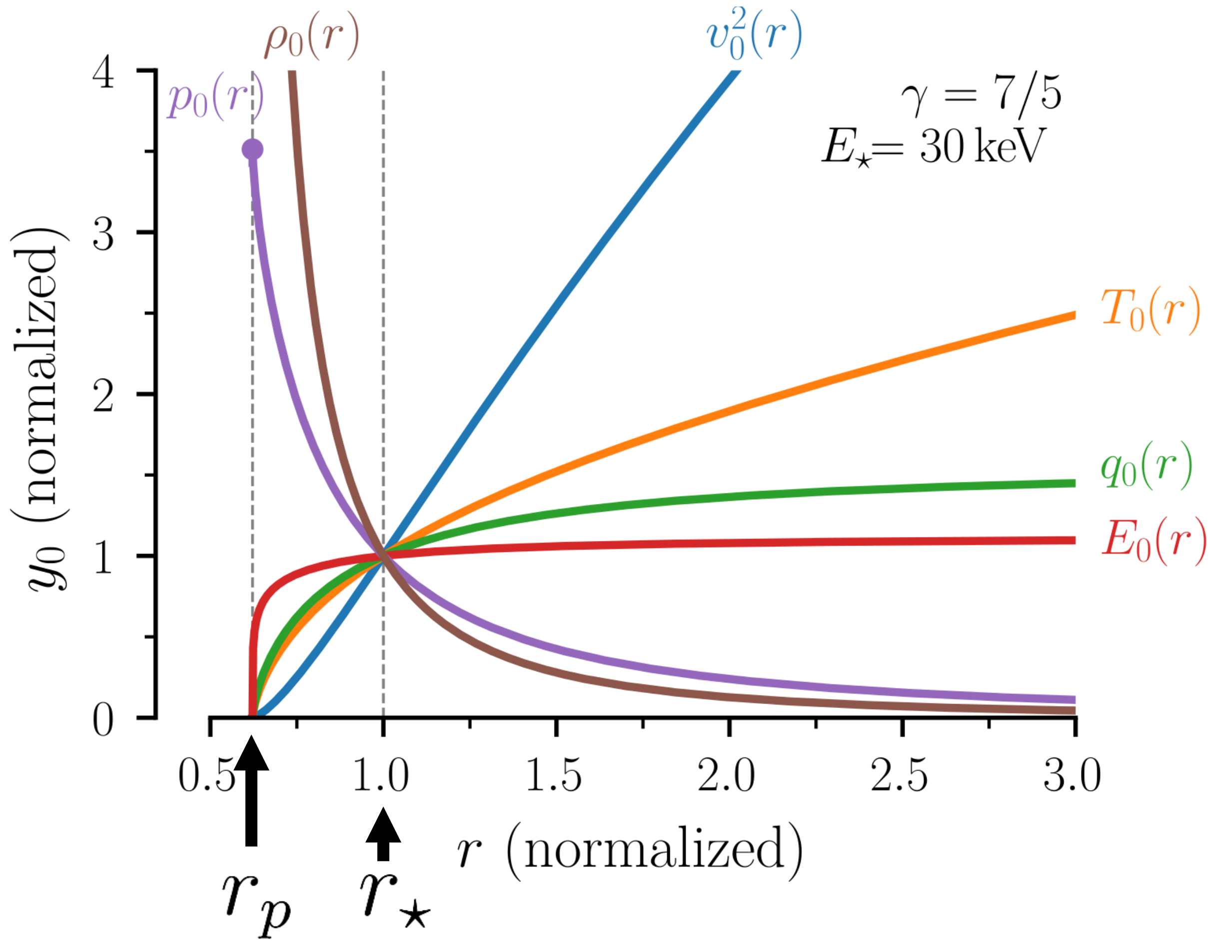

Isotropic NGS scaling laws

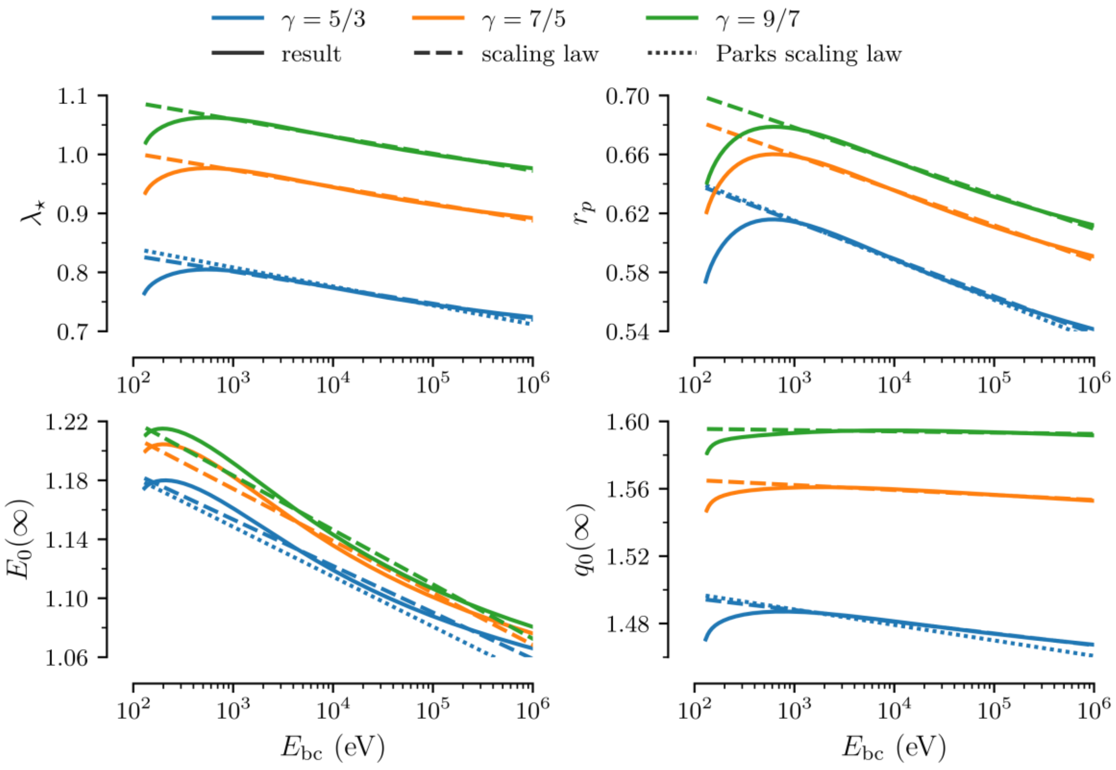

- validates implementation
  - Parks & Turnbull (1977)
- weak E dependence (log-scale!)
- important for rocket effect:

$$\boxed{p_\star = \underbrace{\frac{\lambda_\star}{\gamma}\left(\frac{\tilde{r}_{\rm p}(\gamma-1)^2}{4\tilde{q}^2(\infty)}\right)^{\frac{1}{3}}}_{f_p(E_{\rm bc},\gamma)} \cdot \left[\frac{m(\mu q_{\rm bc})^2}{\Lambda_\star r_{\rm p}}\right]^{\frac{1}{3}}}$$

Outline of solution

- Write in matrix form (algebra using SymPy)

$$\partial\vec{y}_1/\partial r = C(y_0)\vec{y}_1, \qquad \vec{y}_1 = (p_1, T_1, v_{1,r}, v_{1,\theta}, q_1, E_1)^T$$

- Apparent singularity in C at sonic radius
- Enforce continuity => eliminate one unknown

$$\widetilde{v}_{1,\theta}(\widetilde{r}=1) = \left[\left(1-\frac{\chi_\star}{2}\right)\widetilde{v}_{1,r} + \left(1+\frac{\chi_\star}{4}\right)\widetilde{T}_1 - \widetilde{q}_1 - \frac{\partial\widetilde{\Lambda}}{\partial E}\widetilde{E}_1\right]_{\widetilde{r}=1}, \qquad \chi_\star = \partial\widetilde{v}_0^2/\partial\widetilde{r}\big|_{\widetilde{r}=1}$$

- Derivatives at sonic radius from L'Hopitals rule
- Initial value problem starting from sonic radius
- Find remaining unknowns at sonic radius that satisfy BCs

Full NGS solution

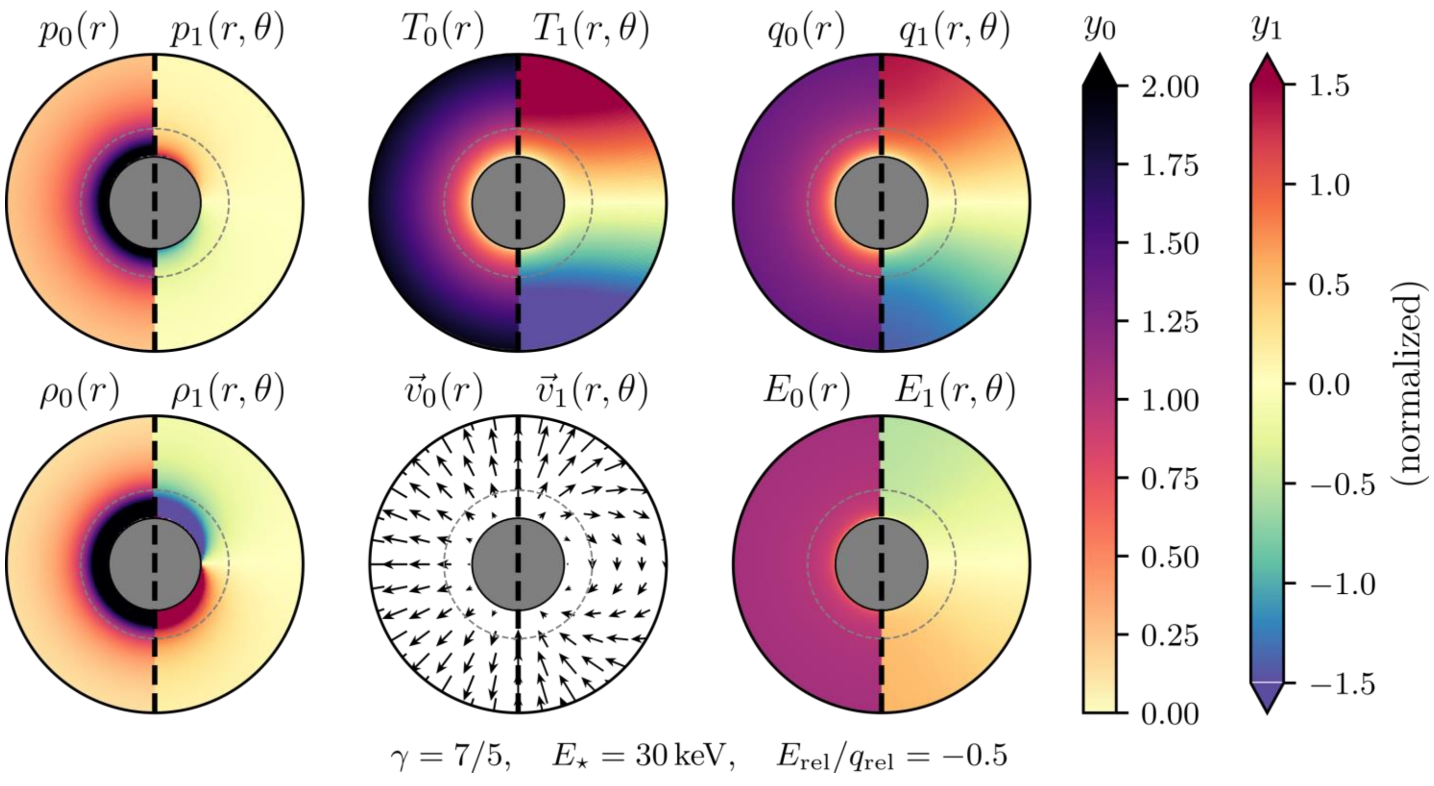

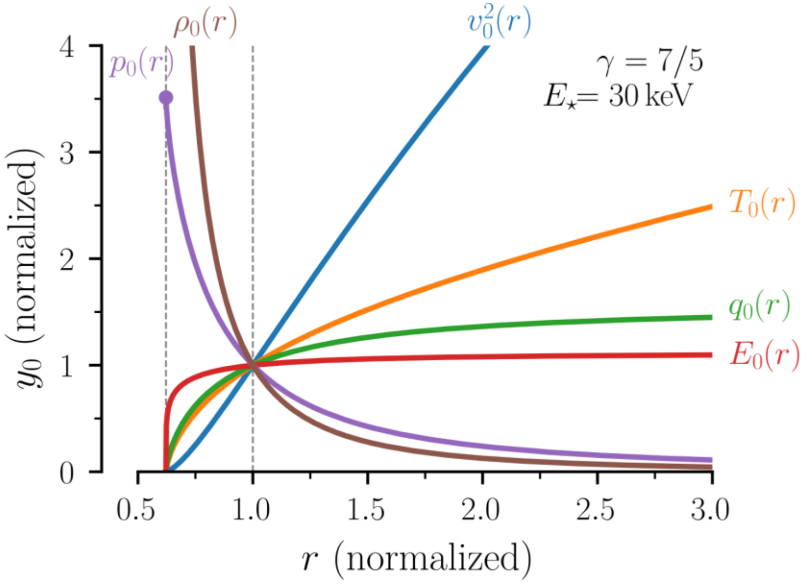

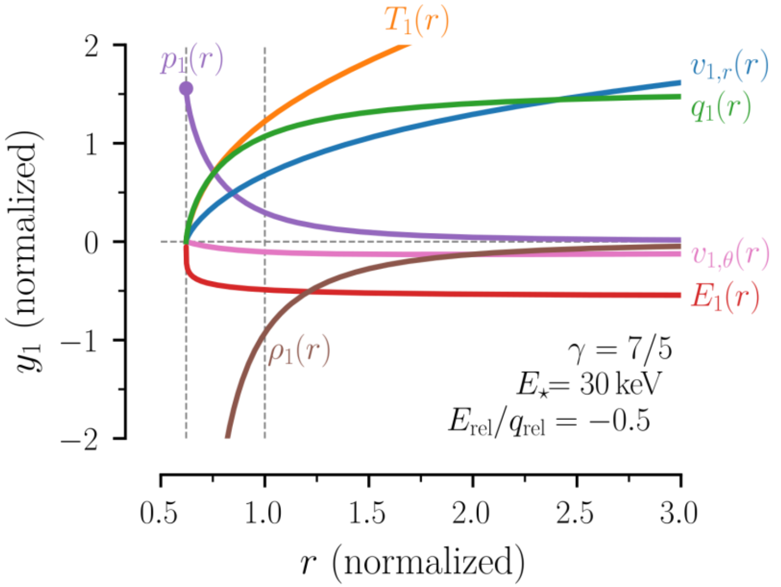

Asymmetric NGS unexpected solutions

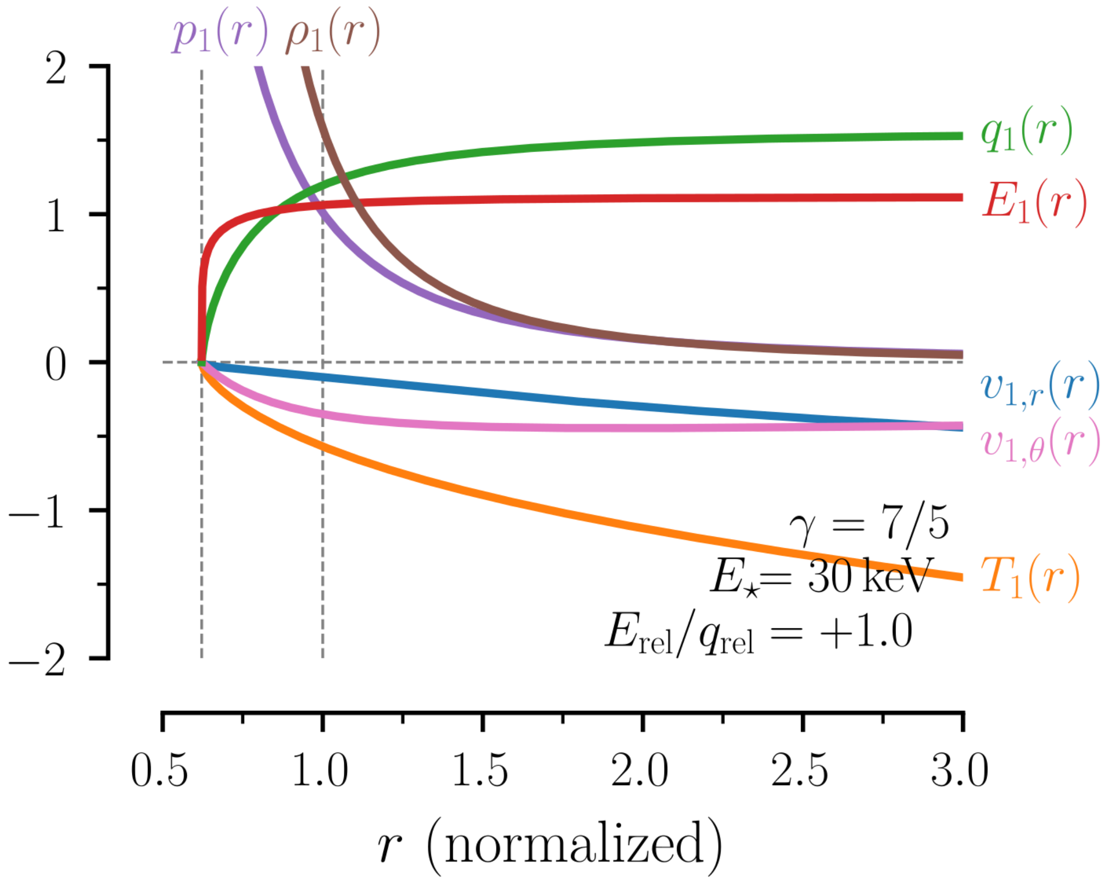

- Temperature higher on less heated side
- Density explains it

Asymmetric NGS unexpected solutions

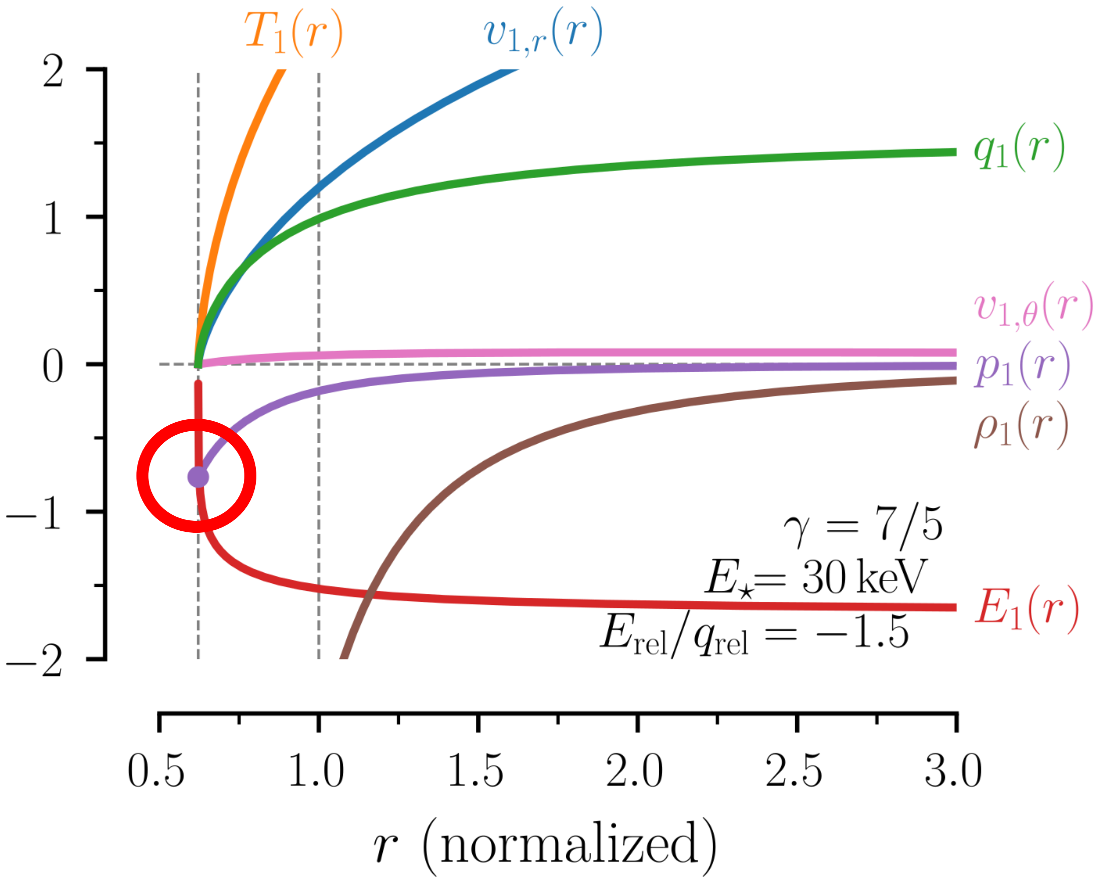

- Pressure higher on less heated side

  → reversed rocket effect
- High-energy electrons
- Not observed experimentally

Plasmoid shielding asymmetry

- Lower energy electrons at less shielded side => negative contribution to E_{rel}
- High energy tail on both sides, lower energy electrons stopped earlier in neutral cloud
  - Not accounted for with monoenergetic beam
  - Energy asymmetry may be underestimated => do calculations also with $E_{\mathrm{rel}}=0$ (upper limit)

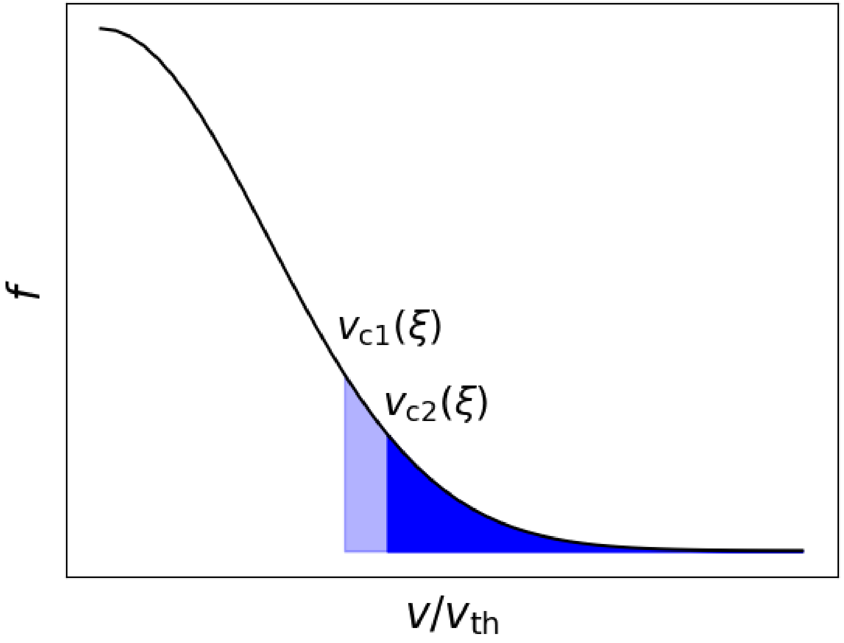

Pressure asymmetry scaling law parameters

$$p_1(r_\mathrm{p}) = a \cdot \left(\frac{E_\mathrm{rel}}{q_\mathrm{rel}} - b\right)$$

$$\boxed{F = \frac{4\pi r_\mathrm{p}^2}{3} p_\star \left(aE_\mathrm{rel} - abq_\mathrm{rel}\right)\ ,}$$

$$\boxed{p_\star = \underbrace{\frac{\lambda_\star}{\gamma}\left(\frac{\tilde{r}_\mathrm{p}(\gamma-1)^2}{4\tilde{q}^2(\infty)}\right)^{\frac{1}{3}}}_{f_p(E_\mathrm{bc},\gamma)} \cdot \left[\frac{m(\mu q_\mathrm{bc})^2}{\Lambda_\star r_\mathrm{p}}\right]^{\frac{1}{3}}}$$

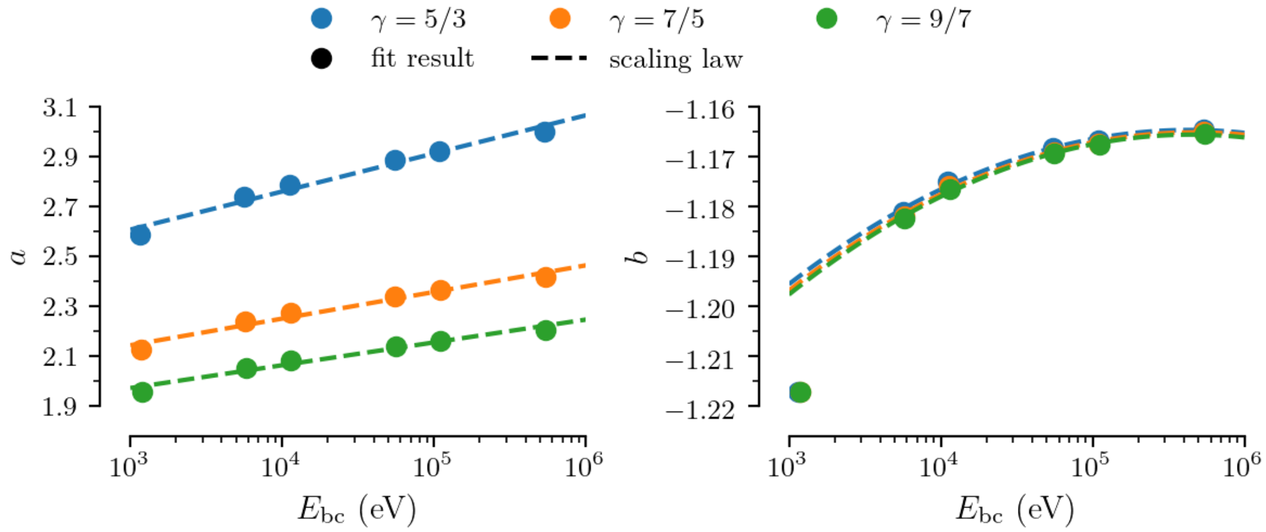

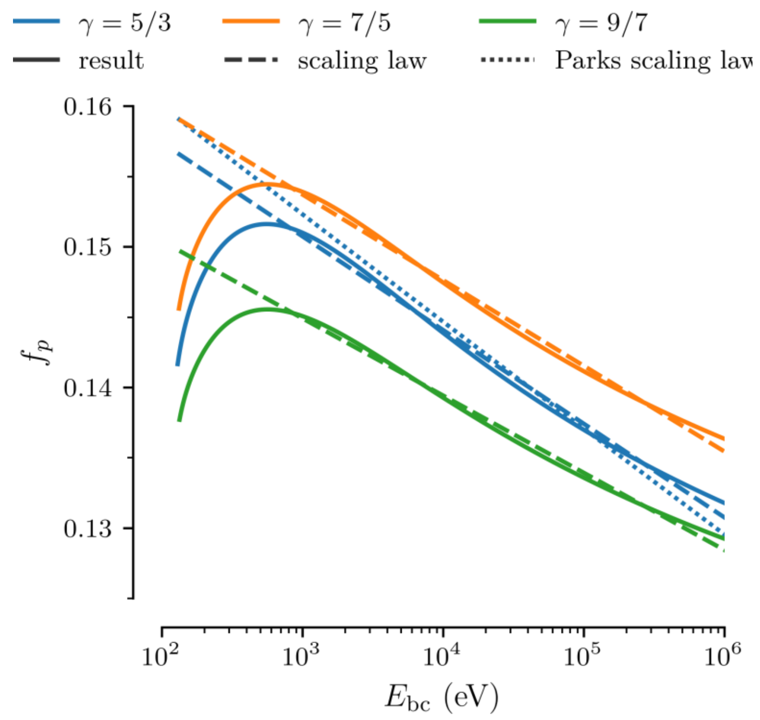

Ablation asymmetry at pellet surface

Relative contribution to the rocket force:

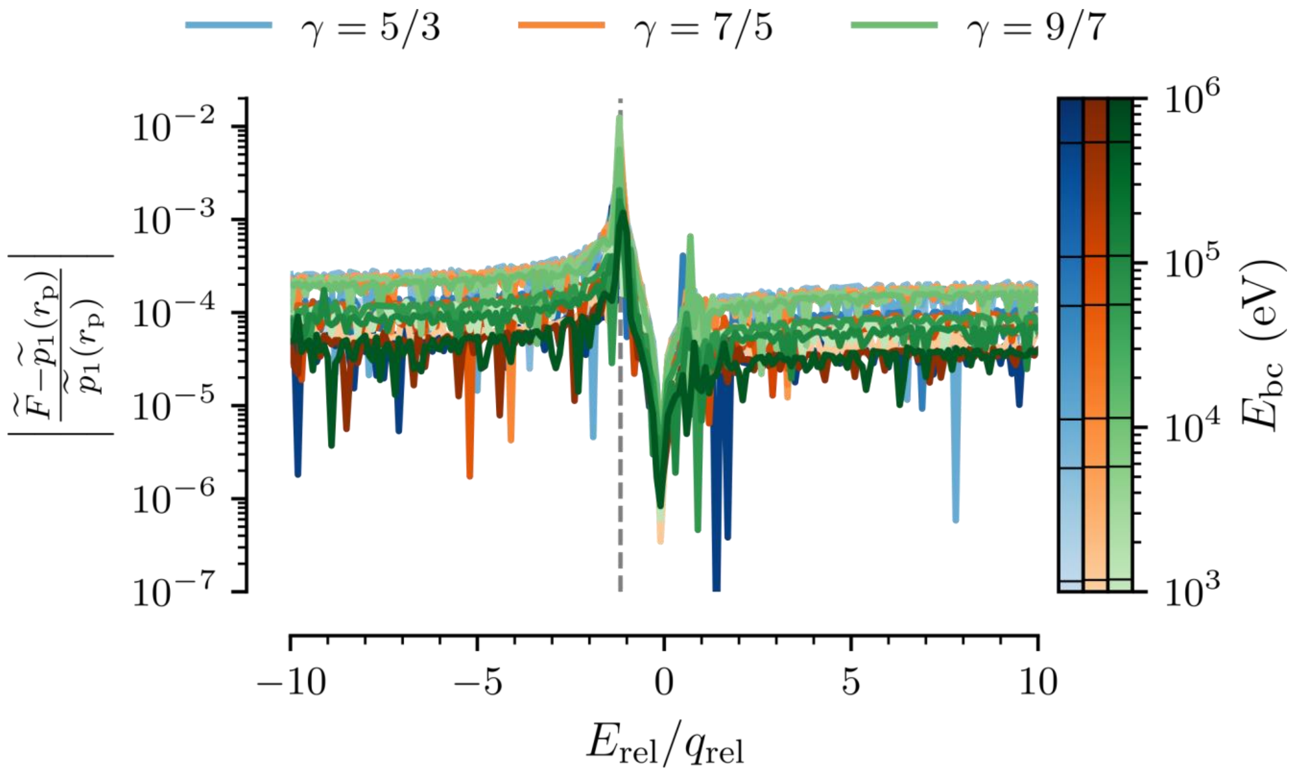

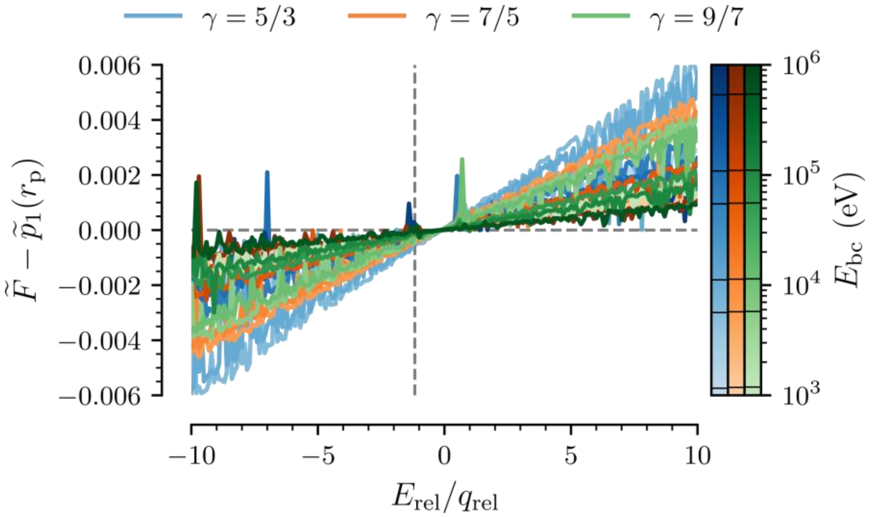

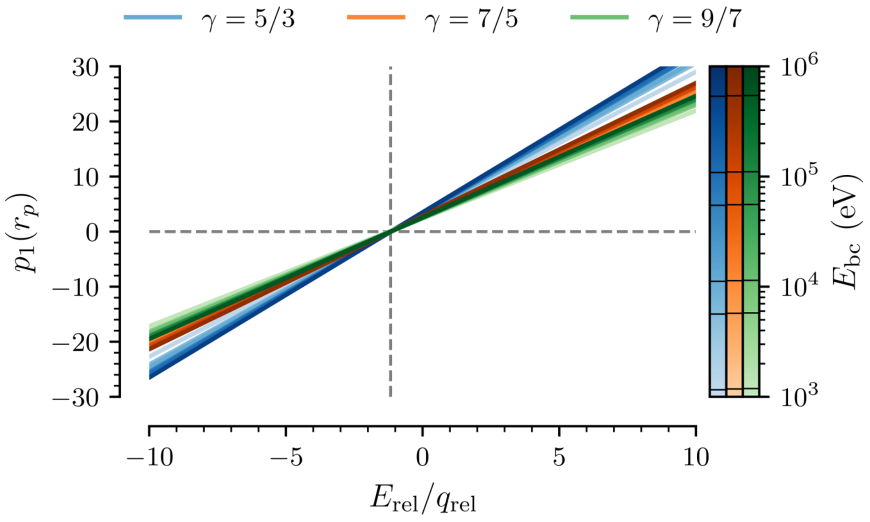

Plasmoid shielding length equations

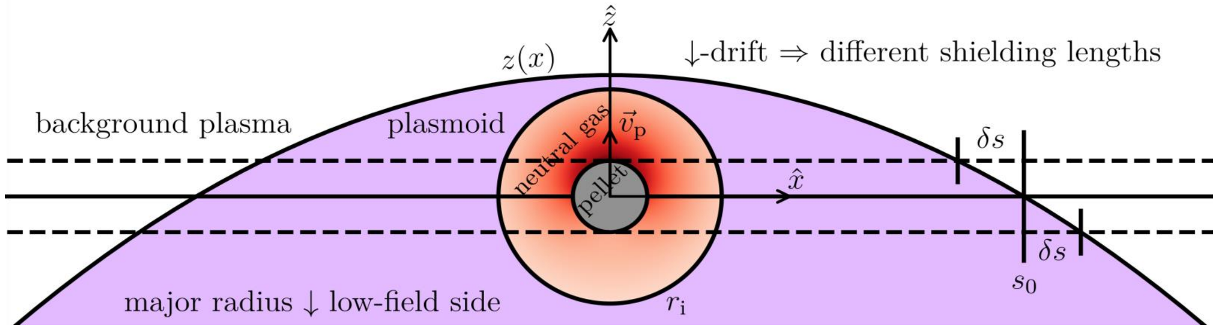

$$\dot{v}_\mathrm{pl} = \frac{2(1+\langle Z\rangle)}{\langle m_i\rangle R_\mathrm{m}}\left(T_\mathrm{pl} - \frac{2n_\mathrm{bg}}{(1+\langle Z\rangle)n_\mathrm{pl}}T_\mathrm{bg}\right)$$

$$\vec{r}(t) = (\pm c_\mathrm{s} t)\hat{x} + \left(r_\mathrm{i} - v_\mathrm{p} t - \frac{1}{2}\dot{v}_\mathrm{pl} t^2\right)\hat{z}$$

$$s(z) = c_\mathrm{s}\left(-\frac{v_\mathrm{p}}{\dot{v}_\mathrm{pl}} + \sqrt{\left(\frac{v_\mathrm{p}}{\dot{v}_\mathrm{pl}}\right)^2 + \frac{2}{\dot{v}_\mathrm{pl}}(r_\mathrm{i} - z)}\right) - \sqrt{r_\mathrm{i}^2 - z^2}\,.$$

$$n_\mathrm{pl} = \frac{\mathcal{G}}{2\langle m_i\rangle c_\mathrm{s}(T_\mathrm{pl})\pi r_\mathrm{i}^2}$$

$$\delta s\,(z) = \left.\frac{\mathrm{d}s}{\mathrm{d}z}\right|_{z=0}\cdot z = \left.\frac{\mathrm{d}s}{\mathrm{d}z}\right|_{z=0}\cdot r_\mathrm{p}\cos\theta\,,$$

$$\left.\frac{\mathrm{d}s}{\mathrm{d}z}\right|_{z=0} = \frac{-c_\mathrm{s}}{\sqrt{v_\mathrm{p}^2 + 2\dot{v}_\mathrm{pl} r_\mathrm{i}}}\,.$$

Plasmoid shielding asymmetry

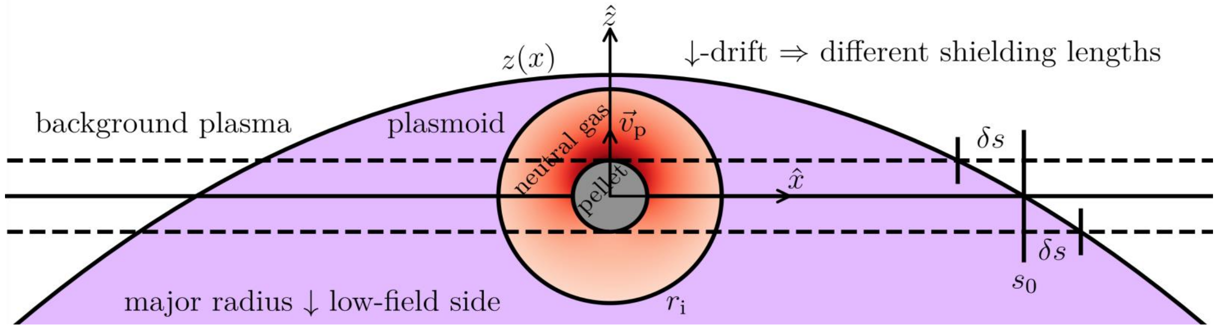

$$E_{\rm pl}(s) = \underbrace{2T_{\rm bg}}_{E_{\rm Parks}} \underbrace{\left[\frac{e^{\frac{-1}{\sqrt{\alpha}}}\left(-\frac{1}{2}\sqrt{\alpha}+\frac{1}{2}\alpha+\alpha^{3/2}+\alpha^2\right)-\frac{1}{2}\mathrm{Ei}\left(-\frac{1}{\sqrt{\alpha}}\right)}{e^{\frac{-1}{\sqrt{\alpha}}}\left(+\frac{1}{2}\sqrt{\alpha}-\frac{1}{2}\alpha+\alpha^{3/2}+\alpha^2\right)+\frac{1}{2}\mathrm{Ei}\left(-\frac{1}{\sqrt{\alpha}}\right)}\right]}_{f_E(\alpha)}$$

$$q_{\rm pl}(s) = \underbrace{2\sqrt{\frac{T_{\rm bg}^3}{2\pi m_e}}n_{\rm bg}}_{q_{\rm Parks}} \underbrace{\frac{1}{\alpha^2}\left[e^{\frac{-1}{\sqrt{\alpha}}}\left(-\frac{1}{2}\sqrt{\alpha}+\frac{1}{2}\alpha+\alpha^{3/2}+\alpha^2\right)-\frac{1}{2}\mathrm{Ei}\left(-\frac{1}{\sqrt{\alpha}}\right)\right]}_{f_q(\alpha)}$$

- isotropic heating:

$$q_{\rm bc} = q_{\rm pl}(s_0) = q_{\rm Parks} f_q(\alpha_0)$$
$$E_{\rm bc} = E_{\rm pl}(s_0) = E_{\rm Parks} f_E(\alpha_0)$$

- asymmetric heating:

$$q_{\rm rel} = r_{\rm p}\left[\left(\frac{3}{2}\frac{1}{T_{\rm bg}}+\frac{f_q'}{f_q}\frac{2\alpha}{\sqrt{T_{\rm bg}}}\right)\frac{\mathrm{d}T_{\rm bg}}{\mathrm{d}z}+\frac{1}{n_{\rm bg}}\frac{\mathrm{d}n_{\rm bg}}{\mathrm{d}z}-\frac{f_q'}{f_q}\frac{\alpha}{s}\frac{\mathrm{d}s}{\mathrm{d}z}\right]_{z=0}$$

$$E_{\rm rel} = r_{\rm p}\left[\left(\frac{1}{T_{\rm bg}}+\frac{f_E'}{f_E}\frac{2\alpha}{\sqrt{T_{\rm bg}}}\right)\frac{\mathrm{d}T_{\rm bg}}{\mathrm{d}z}-\frac{f_E'}{f_E}\frac{\alpha}{s}\frac{\mathrm{d}s}{\mathrm{d}z}\right]_{z=0}$$

$$\alpha := \lambda_T/s$$

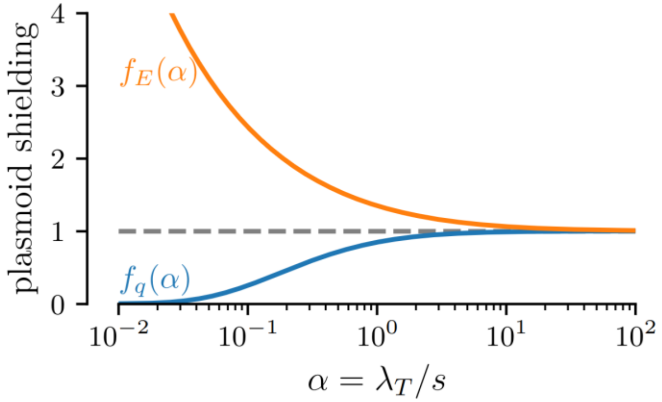

Pellet trajectory simulation in AUG

- Coupled ablation rate and rocket force equations
- Fix background plasma profiles
  - Material drifts away from pellet
- Profiles similar to Szepesi et al, Journal of Nucl. Mat. 2009

  $\#23078, \quad T_{\max} \approx 0.6\,\mathrm{keV}, \quad n_{\max} \approx 10^{20}\,\mathrm{m}^{-3}$
- Result sensitive to ionization radius scale factor f_{ri}, but agrees with experiment with $f_{\mathrm{ri}} \approx 1$

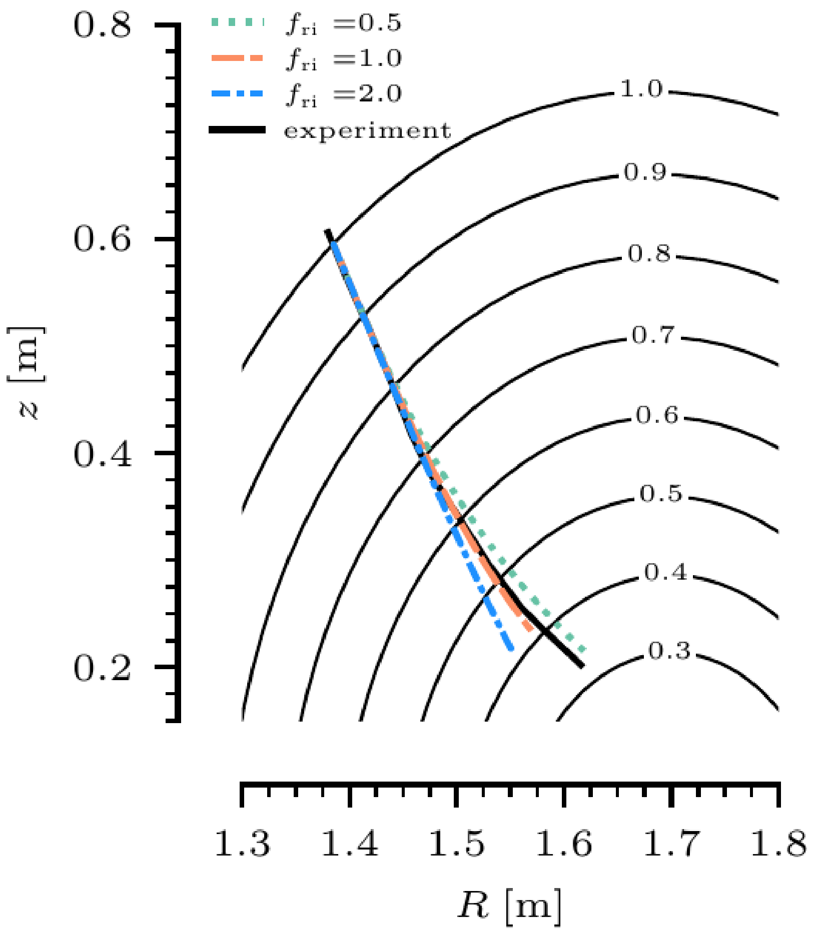

Penetration depth in medium sized tokamaks

- Coupled ablation rate and rocket force equations
- Fix background plasma profiles
  - Material drifts behind pellet
- Profiles similar to Müller et al NF 2002

$T_{\mathrm{max}} = 2\,\mathrm{keV} \qquad n_{\mathrm{max}} = 5 \cdot 10^{19}\,\mathrm{m}^{-3}$

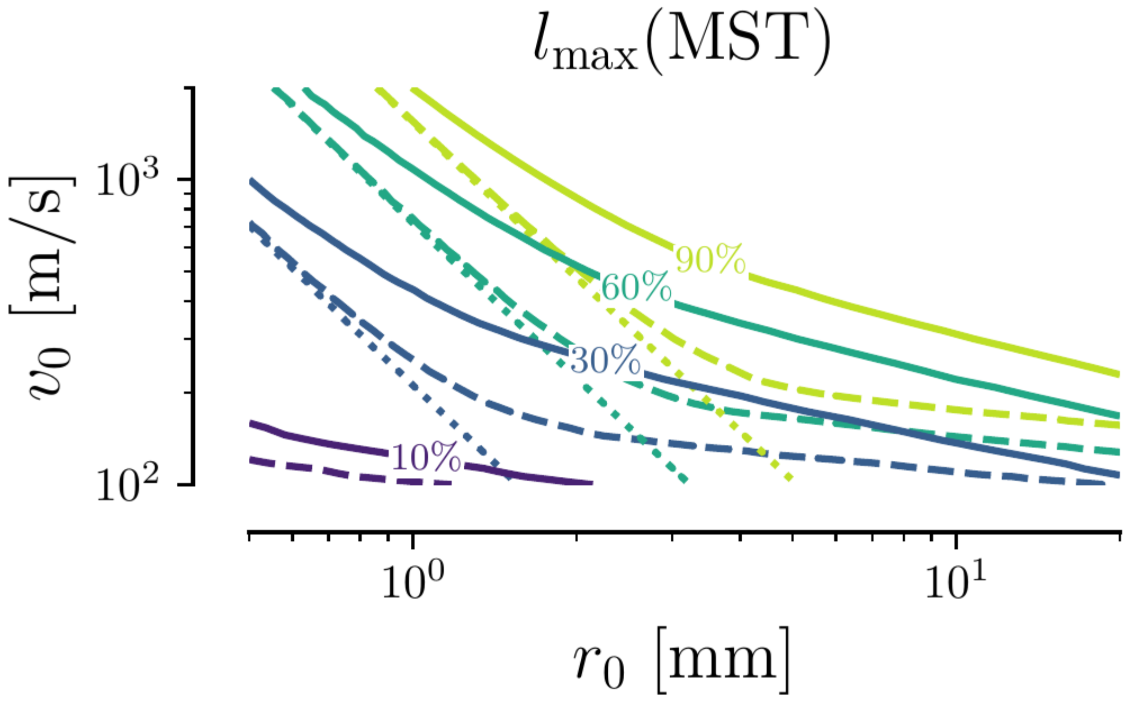

Referenced publications

Parks, P. B., & Turnbull, R. J. (1978). Effect of transonic flow in the ablation cloud on the lifetime of a solid hydrogen pellet in a plasma. The Physics of Fluids, 21(10), 1735–1741. https://doi.org/10.1063/1.862088

Samulyak, R. (2023). Simulation study of the influence of grad-B drift on pellet ablation dynamics. Theory and Simulation of Disruptions Workshop, Princeton Plasma Physics Laboratory. https://tsdw.pppl.gov/Talks/2023/Samulyak.pdf

Senichenkov, I., Rozhansky, V., & Gusakov, P. (2007). The pellet rocket acceleration caused by B-induced drift. Europhysics Conference Abstracts, 31F, P4.094. https://info.fusion.ciemat.es/OCS/EPS2007/pdf/P4_094.pdf

Szepesi, T., Kálvin, S., Kocsis, G., & Lang, P. T. (2007). Radial acceleration of solid hydrogen pellets in hot tokamak plasmas. 34th EPS Conference on Plasma Physics, 31F, P.4037. https://info.fusion.ciemat.es/OCS/EPS2007/pdf/P4_037.pdf

Szepesi, T., Kálvin, S., Kocsis, G., & Lang, P. T. & Senichenkov, I (2009). Comparison of pellet acceleration model results to experimentally observed penetration depths. Journal of Nuclear Materials, 390-391, 507-510. https://doi.org/10.1016/j.jnucmat.2009.01.063